ISSN 0016-7932, Geomagnetism and Aeronomy, 2023, Vol. 63, No. 1, pp. 105–112. © Pleiades Publishing, Ltd., 2023.

The Geomagnetic Regional Model in Indonesia for Epoch 2020.0

Muhamad Syirojudin[a, b], Eko Haryono[c], Suaidi Ahadi[b, *], Suko Prajitno Adi[b], and Noor Efendi[b]

[a] *Doctoral Program in Geography, Gadjah Mada University, Yogyakarta, Indonesia*

[b] *Meteorological, Climatological, and Geophysical Agency, Jakarta, 10720 Indonesia*

[c] *Department of Environmental Geography, Gadjah Mada University, Yogyakarta, Indonesia*

**e-mail: suaidi.ahadi@bmkg.go.id*

Received October 14, 2022; revised January 24, 2023; accepted January 26, 2023

Abstract—The geomagnetic field at the earth's surface changes over time, including in Indonesia. An accurate regional geomagnetic model is needed. Indonesia conducted just 49 repeat station measurements (out of 68) in epoch 2020.0 due to the COVID-19 pandemic. The regional geomagnetic field was modeled using the collocated cokriging (CC) method, which is proven to be accurate. The results show high accuracy with 1.18 minutes root mean square error (RMSE) for the declination component (D), 11.1 minutes for the inclination component (I), and 36.6 nT for the total intensity component (F). This RMSE indicates a similar result to epoch 2015.0. It is apparent that the problem of fewer data for epoch 2020.0 has been solved using the CC method. The crustal geomagnetic fields are also modeled by combining repeat station data and an enhanced magnetic model (EMM). The crustal field model illustrates that 94% of repeat stations exist in the low values, contributing to global geomagnetic modeling in the future. The low crustal field values have also correlated with great earthquake epicenters (magnitude ≥6). The earthquakes occurred in the crustal field values under 120 nT from 2010 to 2020.

Keywords: collocated cokriging, Epoch 2020.0, geomagnetic, Indonesia, repeat station

DOI: 10.1134/S001679322260062X

1. INTRODUCTION

Indonesia is an archipelago with more than 17000 islands and lies longitudinally from 94° to 141° with a wide range of geomagnetic fields. Geomagnetic fields also change over time and this is called secular variation. This variation results from the activities in the earth's internal structure (Alken et al., 2021). A secular variation always changes and is hard to predict in months to millions of years (Geese et al., 2011). Based on this environmental condition, the regional geomagnetic measurement and modeling in the repeat stations are conducted periodically.

Some government and private sectors urgently need an accurate regional geomagnetic model of Indonesia. The economy, research, and mining sectors need a geomagnetic map with a declination accuracy of 0.1° and total intensity accuracy of 50 nT (Macmillan and Rycroft, 2010). The geomagnetic field measurement in Indonesia has been conducted by Badan Meteorologi, Klimatologi dan Geofisika, or Meteorological, Climatological, and Geophysical Agency of Indonesia (BMKG) at the repeat stations every epoch (five years) since 1985.

The geomagnetic field chart in each epoch is produced based on its measurement. The previous epoch (i.e., 2015.0) used 68 repeat stations as the data source. However, due to the COVID-19 pandemic at epoch 2020.0, some repeat stations were not accessible. Hence, only 49 repeat stations were observed and involved in the survey. Those locations involved are evenly distributed across Indonesia, as can be seen in Fig. 1. This decision optimally leveraged the limited locations to produce a good regional geomagnetic model.

All the repeat stations are in airport areas. Airports are accessible and vast, so it is easy to find a location isolated from electromagnetic noise. They are also available for a long period (more than 100 years). They can also be used to calibrate the runway azimuth (Loubser and Newitt, 2009; Rasson and Delipetrov, 2006) to support airport operations. The geomagnetic survey locations in each listed airport were marked by the lightning rod tip at the air traffic control tower, located at a distance more than 200 meters from the station to diminish any electromagnetic noise. The fixed location of the measurement across epochs could support the measurement of the secular variation value.

Regional geomagnetic field modeling needs a different method than global geomagnetic field modeling because the harmonic spherical equation analysis used by global modeling is not suitable for a limited orthogonal area (Mandea and Purucker, 2005). Moreover, the modeling for regional geomagnetic fields for epoch 2020.0 used fewer data than the previous epoch. The

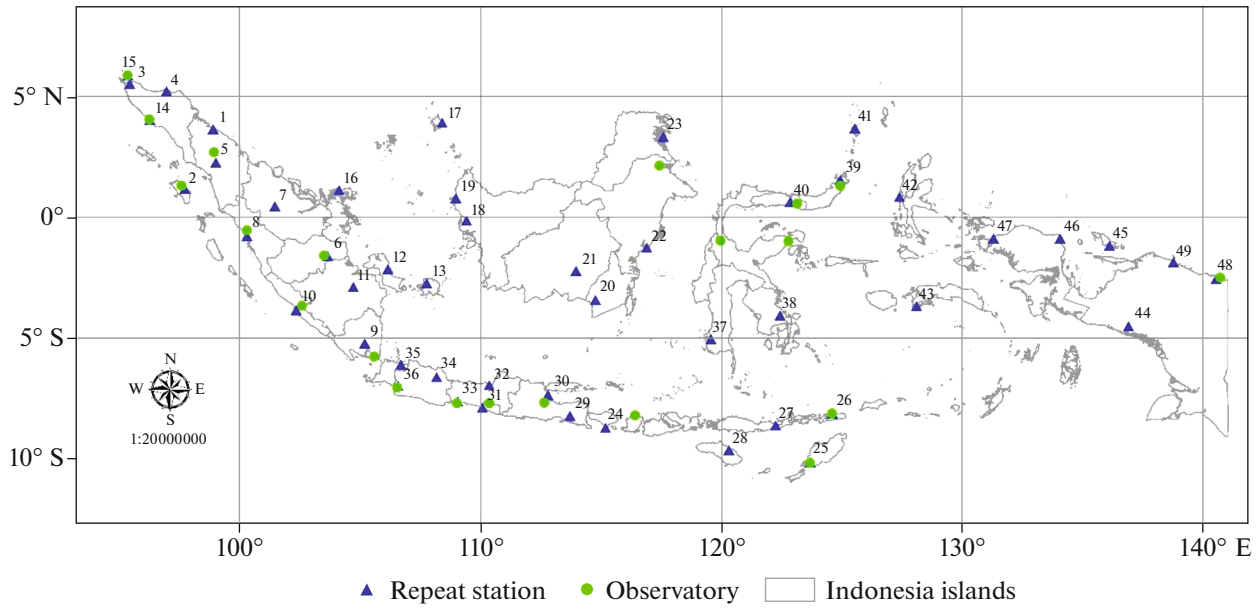

Fig. 1. Distribution of the 49 repeat stations and 21 observatories for epoch 2020.0.

collocated cokriging (CC) method is proven to have enhanced accuracy for Indonesia's regional geomagnetic field modeling (Syirojudin et al., 2022). By using this method, this paper aims to model regional geomagnetic fields for epoch 2020.0 and the crustal geomagnetic field model in Indonesia.

2. DATA AND METHODS

We used the following tools that were already calibrated and used in the survey:

1) The GSM-19T, a proton precision magnetometer, operated on its base station mode with a resolution of 0.01 nT. The accuracy of 0.2 nT is used to measure the geomagnetic field's total intensity component (F).

2) The Mag-01H, a declination inclination magnetometer (DIM) with a resolution of 0.1 nT and a directional accuracy of three seconds, is used to measure the declination (D) and inclination (I) components of the geomagnetic field.

3) The MinGeo 010, a DIM with a resolution of 0.1 nT and a directional accuracy of one second, is also used to measure the D and I components of the geomagnetic field.

4) A GPS Garmin-76 PCX is used to measure the location's longitude, latitude, and elevation.

The theodolite of the DIM is also used to observe the sun and measure the true azimuth (concerning geographic north) to provide the direction reference. The measurement process is based on the international standard from the International Association of Geomagnetism and Aeronomy (Newitt et al., 1996). The measurement is carried out at two periods each day, i.e., the morning and afternoon sessions. Each session fills five data observation forms using the DIM tool and three such forms using the DIM theodolite. Because the range of the D value in Indonesia is quite small, the measurement of the true azimuth reference mark is performed until an accuracy of five seconds in deviation is reached.

Pre-processing is needed before the main analysis because the measurement in a different location is carried out at a different time. The geomagnetic data obtained from the 49 locations are deducted by the diurnal variation data from the 21 observatory stations in Indonesia, followed by a deduction from the secular variation data to produce the epoch 2020.0 figures. The deduction is varied depending on the measurement time and location.

The next step is to process the data using the CC method to produce the geomagnetic figures for epoch 2020.0. CC is a geostatistical method with the best linear unbiased estimator (Webster and Oliver, 2008). It uses two or more variables to estimate the produced data model. In this paper, the geomagnetic data obtained from the survey are used as the primary data, and the main and crustal geomagnetic figures from the enhanced magnetic model (EMM 2017) are used as the secondary data. The following CC equation is used to compute the resulting value (Rivoirard, 2001) as shown in Equation (1).

$$Z_{\mathrm{CC}}(x_0) = \sum_i \lambda_i Z_1(x_i) + \mu Z_2(x_0). \qquad (1)$$

Z_{CC} is the data estimation result of the CC method, λ is the weight of each location in the primary data (repeat station data), Z_1 is the primary data, μ is the

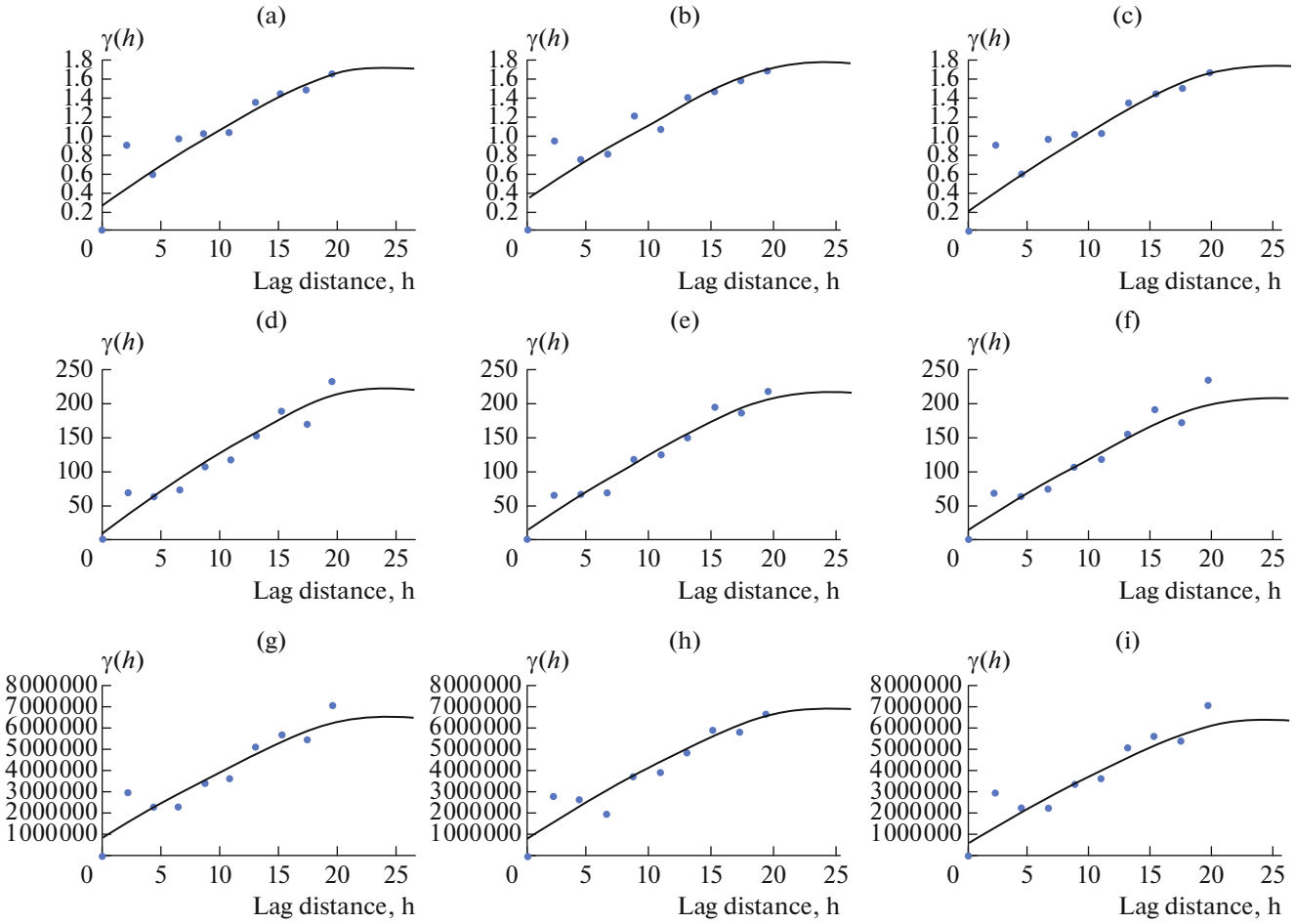

Fig. 2. Semi-variogram of geomagnetic data from epoch 2020.0 for the CC method. Spherical variogram of D component consists of (a) repeat stations as primary data, (b) EMM as secondary data, and (c) primary to secondary data. I component for spherical variogram consists of (d) repeat stations as primary data, (e) EMM as secondary data, and (f) primary to secondary data. F component spherical variogram consists of (g) repeat stations as primary data, (h) EMM as secondary data, and (i) primary to secondary data.

weight of each set of secondary data (EMM 2017), and Z_2 is the secondary data.

The variogram model of both the primary and secondary data is computed to produce their parameter values (the range, sill, and nugget). Three types of variograms (i.e., primary data, secondary data, and cross or primary to secondary) are used for each geomagnetic component. The cross variogram (primary to secondary parameters) used in the CC model is in the range of 3.41, the sill 0.0023, and the nugget 0.0001 for the D component; the range of 27.8, the sill 228.1, and the nugget 10.2 for the I component; and the range of 24.12, the sill 6.3e + 6, and the nugget 6.3e + 5 for the F component as shown in Fig. 2.

The secular variation is computed by subtracting the geomagnetic data of epoch 2020.0 from that of epoch 2015.0, then dividing them by five to get the annual change value. The annual change factor is used to compute and predict each year's geomagnetic values from 2020.0 until 2025.0. However, the geomagnetic values of the six observatories were obtained empirically because they obtained daily measurements throughout the year.

3. RESULTS AND ANALYSIS

3.1. The Effect of Reducing the Number of Repeat Stations

We compared the analysis of reducing the number of repeat stations of the 2020.0 epoch with regional geomagnetic data for computing modeling from the previous epoch (i.e., epoch 2015.0) using the same method. The regional geomagnetic modeling of the 2020.0 epoch using the CC method results in a small root mean square error (RMSE) or σ for each component, i.e., σd = 1.18 minutes for D, σi = 11.1 minutes for I, and σf = 36.6 nT for F. The regional geomagnetic model for epoch 2015.0 resulted in a similar RMSE of

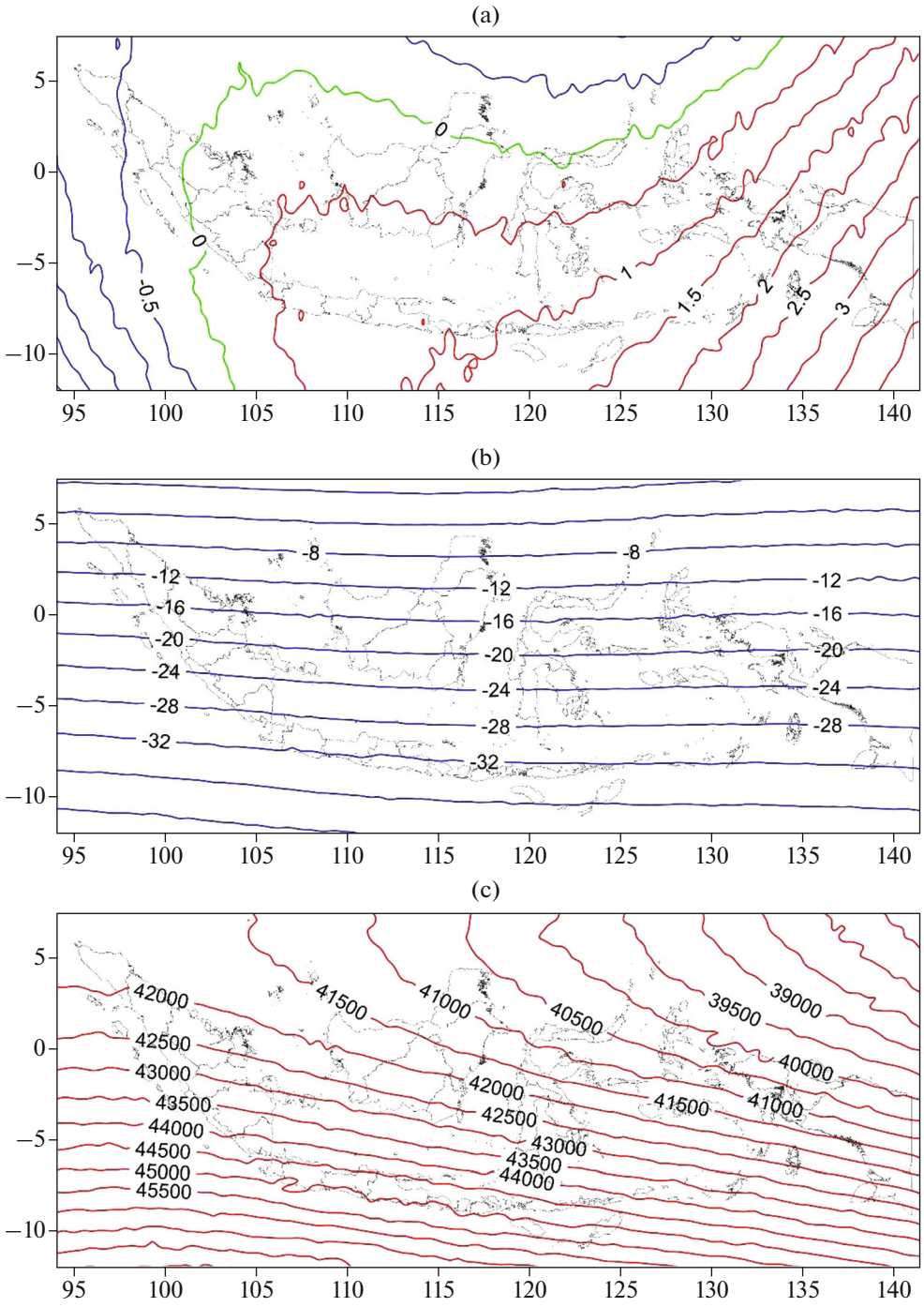

Fig. 3. Geomagnetic chart for epoch 2020.0 using the CC method in Indonesia; (a) D component with $\Delta = 0.5°$, (b) I component with $\Delta = 5°$, and (c) F component with $\Delta = 1000$ nT.

1.05 minutes for D, 10.98 minutes for I, and 35.4 nT for F.

The results show that a decrease in the number of repeat stations involved in the survey at epoch 2020.0 is not significantly different, even though fewer repeat stations were used in 2020.0 (28% fewer stations than the previous epoch). Fewer data in the CC method are compensated by semi-variogram secondary data generated from International Geomagnetic Reference Field (IGRF). Using variograms from secondary data is the advantage of the CC method (Abedi et al., 2015; Rivoirard, 2001). For the D component, the regional geomagnetic model for epoch 2020.0 indicates a RMSE of 0.13 minutes higher than epoch 2015.0. The

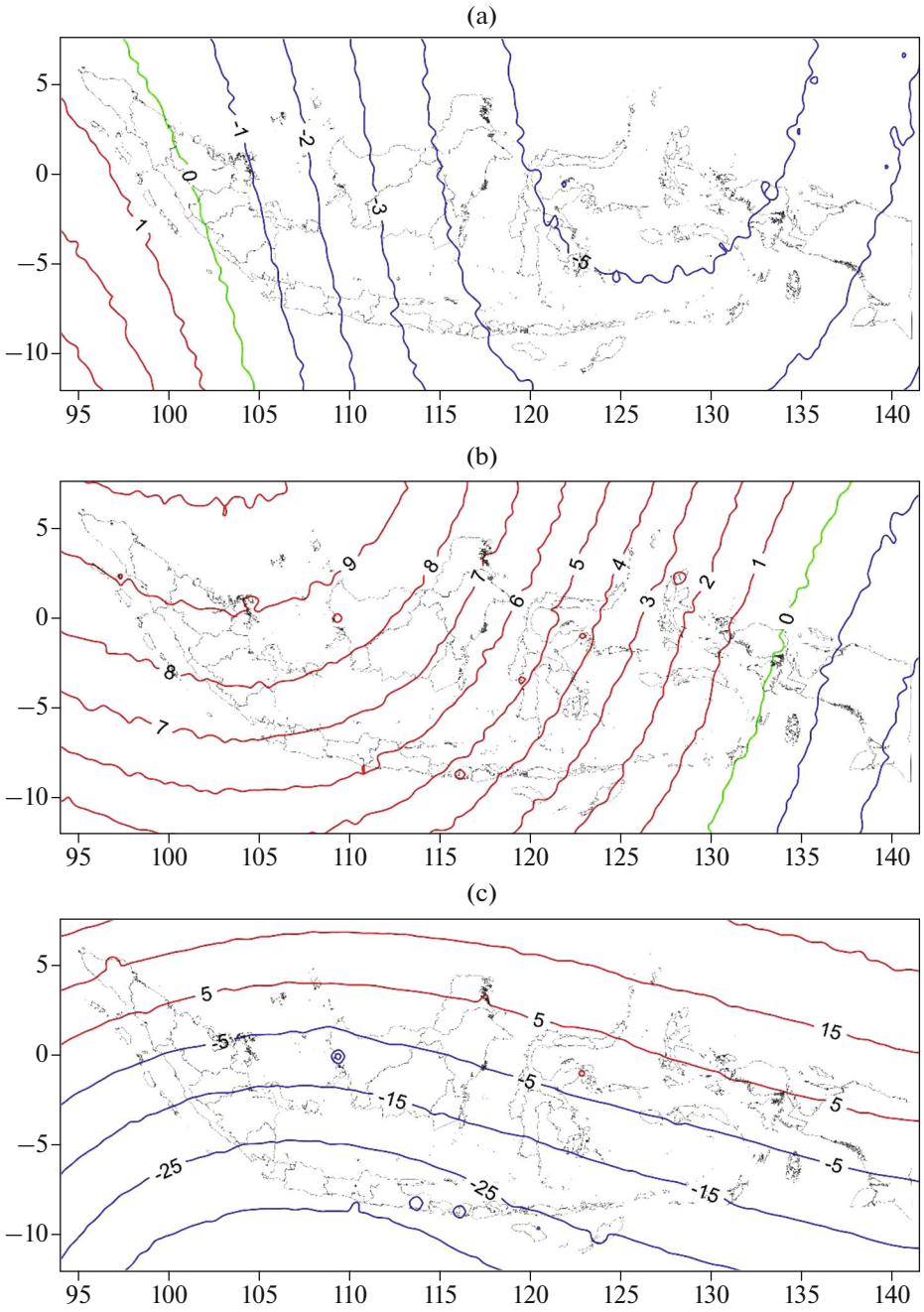

Fig. 4. Secular variation chart for epoch 2020.0 in Indonesia; (a) D component with Δ = 1 minute; (b) I component with Δ = 1 minute; and (c) F component with Δ = 10 nT.

I component's RMSE is 0.12 minutes higher, and the F component's RMSE is 1.2 nT higher than that of the previous epoch. This statement has been proven in our previous research, where the 28% data difference did not significantly affect this method (Syirojudin et al., 2022). The RMSE also still fulfills the required accuracy value in the mining sector, which is 0.1° for the D component and 50 nT for the F component (Macmillan and Rycroft, 2010).

3.2. Regional Geomagnetic and Secular Variation Charts of the 2020.0 Epoch

The regional geomagnetic model of Indonesia varies spatially in latitude and longitude. Indonesia lies from −12° to 8° and 94° to 141°, so it is impossible to have regular or linear variation caused by the dynamic structure under wide regional areas (Heirtzler and Nazarova, 2003; Korte and Lesur, 2012). The resulting regional geomagnetic chart of epoch 2020.0 has more

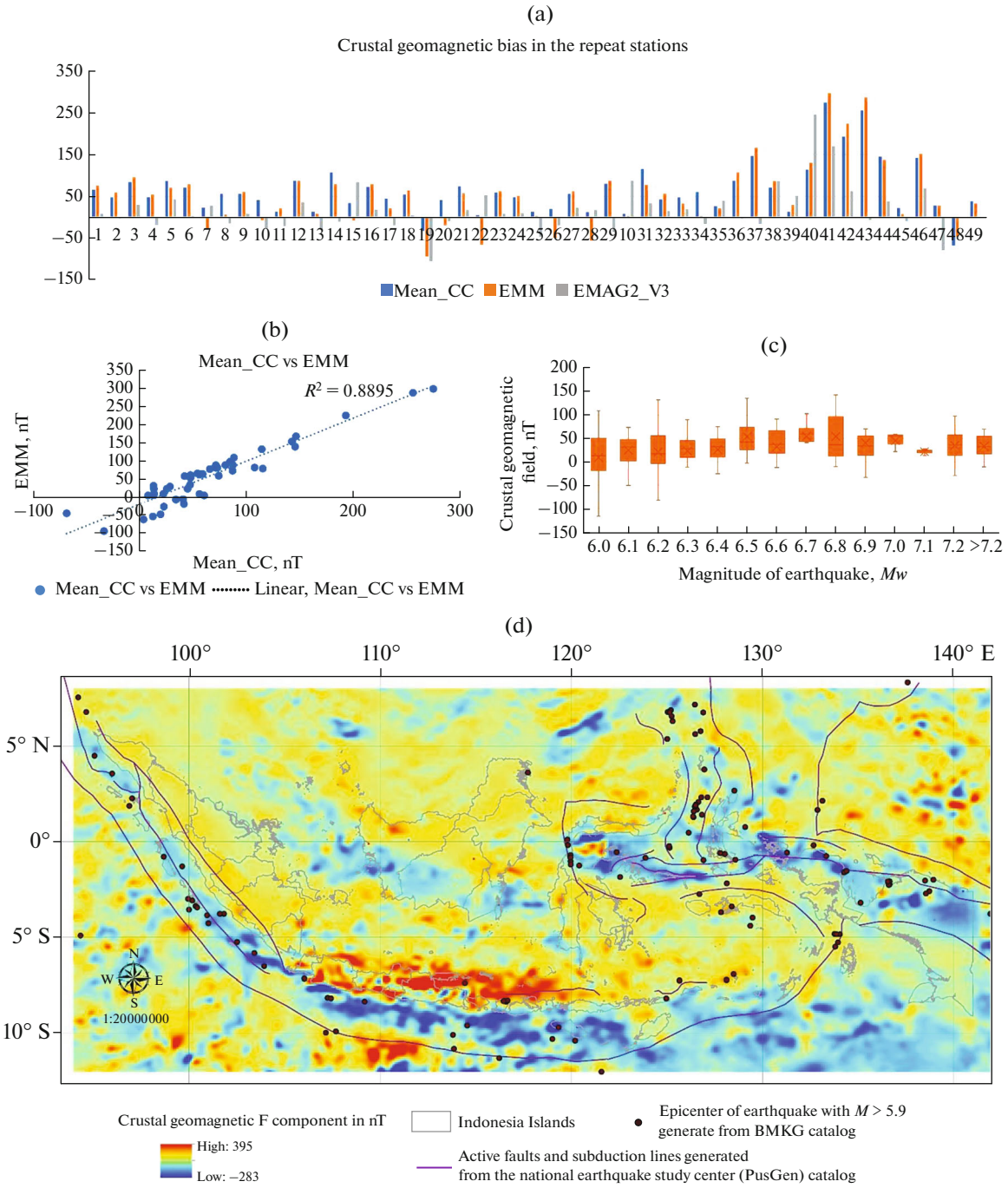

Fig. 5. Crustal field of the geomagnetic F component in Indonesia resulted from the mean of epochs 2010.0, 2015.0, and 2020.0 and correlation with earthquakes; (a) comparing crustal field at repeat station from the CC model, EMM, and earth magnetic anomaly grid 2-arc minutes resolution version-3 (EMAG2_V3) generated from https://www.ncei.noaa.gov/access/metadata/landing-page/bin/iso?id=gov.noaa.ngdc.mgg.geophysical_models:EMAG2_V3, (b) correlation crustal field between CC model and EMM, (c) boxplot of earthquake data from 2010 to 2020 with magnitude (M) ≥ 6 and crustal field, and (d) crustal of the geomagnetic field and earthquake epicenter in Indonesia.

detail than the global model provided in Fig. 3. It is caused by the global model typically limited by the accuracy and the resolution (Maus et al., 2005). Moreover, the global model uses only a small number of observatory stations in Indonesia, i.e., KPG, PLR, TND, and TUN (Alken et al., 2021). The D component in Indonesia is distributed along the longitude and has zero value. It divides into two regions, positive values eastward (from the middle to eastern Indonesia) and negative values westward (in western Indonesia). The I component in the whole of Indonesia provides the negative values with a straight-line contour.

The F component of the geomagnetic measurement has distribution along latitude with positive values from 39000 to 46000 nT.

The secular variation modeling using the CC method specifies a RMSE of 0.03 minutes at the D component, 0.06 minutes at I, and 0.1 nT at F. The secular variation isolines are depicted in Fig. 4. The resulting secular variation data show that Indonesia has a small value change. Any considerable weakening of the geomagnetic values was not observed as the same result in the Pacific region (Yukutake and Shimizu, 2018). An example of a significantly weakened geomagnetic value was observed in the south Atlantic and southern African regions (Finlay et al., 2016). The secular variation model confirms the global model of the IGRF-12. Most of the area in the resulting regional model expresses a negative secular variation value of the D component. However, the western region indicates positive secular variation values, while the eastern region specifies negative secular variation values of the I component. All regions provide positive values for the F component, with the northwest as its greatest value.

3.3. Crustal Geomagnetic Field of Indonesia

We also computed the resulting regional geomagnetic model's discrepancy with the global geomagnetic model (i.e., the IGRF-12) to model the crustal field bias by calculating mean data values from the three latest epochs (2010.0, 2015.0, and 2020.0). The crustal field model resulting from the CC method shows favorable accuracy with a RMSE value of 1.74 nT and high correlation with EMM (R^2 values 0.8895) as given in Fig. 5b.

The crustal field indicated that 94% of the repeat stations exist in low crustal field values, and only three repeat stations (i.e., Naha, Ternate, and Ambon) have crustal field values above 150 nT for the F component as shown in Fig. 5a. This information has contributed considerably to the global model (i.e., IGRF), which models the main field only (Finlay et al., 2010; Maus et al., 2005; Thébault et al., 2015) and needs to remove the crustal geomagnetic field (Korte and Lesur, 2012; Maus, 2008). The three repeat stations with high crustal fields exist in the triple junction of the tectonic and small islands with active volcanoes (i.e., Naha and Ternate) and Paleozoic formations, i.e., Ambon (Darman, 2000; Katili, 1975; Verstappen, 2014).

The spatial distribution of the crustal field is caused by the properties of magnetized rocks below the Curie temperature (Thébault et al., 2010). The crustal field of the F component varies spatially from –280 to 320 nT as shown in Fig. 5d. The low value distribution of the crustal field correlates with the earthquakes that occurred in this region. As shown in Figs. 5c, 5d, the great earthquakes took place from 2010 to 2020 in the crustal field value under 120 nT. The subduction zone and fault line have a low crustal field caused by frictional heating (Mishima et al., 2009) and partial melting (Krien and Fleitout, 2008; Garnero et al., 2016) in this area. During the earthquake cycle, the collision of two layers of rock in the seismogenic zone raise the Curie temperature (Chester, 1994; Scholz, 1998) and decrease crustal magnetization (Gao et al., 2015). When rock reaches a threshold temperature, it melts, encouraging more movement and friction to produce a wider melting area (Behr and Platt, 2014). This process continues until the rock elasticity limit is reached in the seismogenic zone and an earthquake occurs (Wang and Barbot, 2020).

4. CONCLUSIONS

This study analyzes the repeat station measurements for the 2020.0 epoch and data from the three latest epochs to explore the accuracy of the regional geomagnetic field for the 2020.0 epoch and the crustal geomagnetic field in Indonesia. The following conclusions were reached.

(1) The fewer repeat station data for the 2020.0 epoch still resulted in high accuracy with a small RMSE in each component and did not significantly differ from the previous epoch. <...>

(2) The regional geomagnetic and secular variation charts for the 2020.0 epoch are more detailed than the global model and vary spatially in latitude and longitude. <...>

(3) 94% of the repeat stations exist in low crustal field values. <...>

(4) The low crustal field correlates with the great earthquake epicenter that occurred in Indonesia. <...>

ACKNOWLEDGMENTS

We thank the BMKG for supporting and granting access to repeat station data used in this research. We also thank the Geophysical Stations of Deliserdang, Tangerang, Bandung, Kupang, Manado, and Jayapura for supporting the data measurement survey in the repeat stations.

FUNDING

This research was supported and funded by BMKG.

CONFLICTS OF INTEREST

The authors declare that they have no conflicts of interest.

REFERENCES

Abedi, M., Asghari, O., and Norouzi, G.-H., Collocated cokriging of iron deposit based on a model of magnetic susceptibility: A case study in Morvarid mine, Iran. *Arab. J. Geosci.*, 2015, vol. 8, no. 4, pp. 2179–2189. https://doi.org/10.1007/s12517-014-1282-5

Alken, P., Thébault, E., Beggan, C.D., et al., International Geomagnetic Reference Field: The thirteenth generation, *Earth Planets Space*, 2021, vol. 73, no. 1. https://doi.org/10.1186/s40623-020-01288-x

Behr, W.M. and Platt, J.P., Brittle faults are weak, yet the ductile middle crust is strong: Implications for lithospheric mechanics, *Geophys. Res. Lett.*, 2014, vol. 41, pp. 8067–8075. https://doi.org/10.1002/2014GL061349

Chester, F.M., Effects of temperature on friction: Constitutive equations and experiments with quartz gouge, *J. Geophys. Res.*, 1994, vol. 99, no. 93, pp. 7247–7261.

Darman, H., *An Outline of the Geology of Indonesia*, Darman, H. and Sidi, F.H., Eds., Indonesian Geologist Association, 2000.

Finlay, C.C., Maus, S., Beggan, C.D., et al., Evaluation of candidate geomagnetic field models for IGRF-11, *Earth Planets Space*, 2010, vol. 62, no. 10, pp. 787–804. https://doi.org/10.5047/eps.2010.11.005

Finlay, C.C., Olsen, N., Kotsiaros, S., et al., Recent geomagnetic secular variation from Swarm and ground observatories as estimated in the CHAOS-6 geomagnetic field model, *Earth Planets Space*, 2016, vol. 68, no. 1. https://doi.org/10.1186/s40623-016-0486-1

Gao, G., Kang, G., Bai, C., et al., Study on crustal magnetic anomalies and Curie surface in Southeast Tibet, *Asian J. Earth Sci.*, 2015, vol. 97, pp. 169–177. https://doi.org/10.1016/j.jseaes.2014.10.035

Garnero, E.J., McNamara, A.K., and Shim, S.H., Continent-sized anomalous zones with low seismic velocity at the base of Earth's mantle, *Nat. Geosci.*, 2016, vol. 9, no. 7, pp. 481–489. https://doi.org/10.1038/ngeo2733

Geese, A., Korte, M., Kotze, P.B., et al., Southern African geomagnetic secular variation from, 2005 to 2009, *South Afr. J. Geol.*, 2011, vol. 114, nos. 3–4, pp. 515–524. https://doi.org/10.2113/gssajg.114.3-4.515

Heirtzler, J.R. and Nazarova, K., Geomagnetic secular variation in the Indian Ocean, *Earth Planet. Sci. Lett.*, 2003, vol. 207, nos. 1–4, pp. 151–158. https://doi.org/10.1016/S0012-821X(02)01128-7.

Katili, J.A., Volcanism and plate tectonics in the Indonesian island arcs, *Tectonophysics*, 1975, vol. 26, no. 3, pp. 165–188. https://doi.org/https://doi.org/10.1016/0040-1951(75)90088-8

Korte, M. and Lesur, V., Repeat station data compared to a global geomagnetic field model, *Ann. Geophys.*, 2012, vol. 55, no. 6, pp. 1101–1111. https://doi.org/10.4401/ag-5410

Krien, Y. and Fleitout, L., Gravity above subduction zones and forces controlling plate motions, *J. Geophys. Res.*, 2008, vol. 113, no. 9, pp. 1–20. https://doi.org/10.1029/2007JB005270

Loubser, L. and Newitt, L., *Guide for Calibrating a Compass Swing Base*, Hermanus: International Association of Geomagnetism and Aeronomy, 2009, pp. 1–35.

Macmillan, S. and Rycroft, M.J., The Earth's magnetic field, in *Encyclopedia of Aerospace Engineering*, John Wiley and Sons, 2010, pp. 1–12. https://doi.org/10.1002/9780470686652.eae322.

Mandea, M. and Purucker, M., Observing, modeling, and interpreting magnetic fields of the solid earth, *Surv. Geophys.*, 2005, vol. 26, no. 4, pp. 415–459. https://doi.org/10.1007/s10712-005-3857-x

Maus, S., The geomagnetic power spectrum, *Geophys. J. Int.*, 2008, vol. 174, pp. 135–142. https://doi.org/10.1111 /j.1365-246X.2008.03820.x.

Maus, S., Macmillan, S., Chernova, T., et al., The 10th generation international geomagnetic reference field, *Phys. Earth Planet. Inter.*, 2005, vol. 151, nos. 3–4, pp. 320–322. https://doi.org/10.1016/j.pepi.2005.03.006

Mishima, T., Hirono, T., Nakamura, N., et al., Changes to magnetic minerals caused by frictional heating during the 1999 Taiwan Chi-Chi earthquake, *Earth Planets Space*, 2009, vol. 61, pp. 797–801. https://doi.org/10.1186/BF03353185

Newitt, L.R., Barton, C.E., and Bitterly, J., *Guide for Magnetic Repeat Station Surveys*, International Association of Geomagnetism and Aeronomy, 1996.

Rasson, J. L., and Delipetrov, T., Geomagnetics for aeronautical safety: A case study in and around the Balkans, in *NATO Security through Science Series C: Environmental Security*, Springer, 2006.

Rivoirard, J., Which models for collocated cokriging?, *Math. Geol.*, 2001, vol. 33, no. 2, pp. 117–128.

Scholz, C.H., Earthquakes and friction laws, *Nature*, 1998, vol. 391, pp. 37–42.

Syirojudin, M., Haryono, E., and Ahadi, S., The accuracy of geostatistics for regional geomagnetic modeling in an archipelago setting, *Sci. Rep.*, 2022, pp. 1–10. https://doi.org/10.1038/s41598-022-10362-1

Thébault, E., Purucker, M., Whaler, K.A., et al., The magnetic field of the Earth's lithosphere, *Space Sci. Rev.*, 2010, vol. 155, pp. 95–127. https://doi.org/10.1007/s11214-010-9667-6

Thébault, E., Finlay, C.C., Beggan, C.D., et al., International Geomagnetic Reference Field: The 12th generation, *Earth Planets Space*, 2015, vol. 67, no. 1, p. 79. https://doi.org/10.1186/s40623-015-0228-9

Verstappen, H., Indonesian landforms and plate tectonics, *Indones. J. Geosci.*, 2014, vol. 5. https://doi.org/10.17014/ijog.5.3.197-207

Wang, L. and Barbot, S., Excitation of San Andreas tremors by thermal instabilities below the seismogenic zone, *Sci. Adv.*, 2020, vol. 6, no. 36, pp. 1–10. https://doi.org/10.1126/sciadv.abb2057

Webster, R. and Oliver, M.A., *Geostatistics for Environmental Scientists,* John Wiley and Sons, 2008. https://doi.org/10.1002/9780470517277.

Yukutake, T. and Shimizu, H., On the geomagnetic secular variation in the Pacific region, *Phys. Earth Planet. Inter.*, 2018, vol. 283, pp. 122–130. https://doi.org/10.1016/j.pepi.2018.08.008